Coherent DiLL for Direction of Arrival Estimation

Dongyoun Seo*, Seunghyun Min, Kwang Bok Lee, and Yong-Hwan Lee

*LG R&D, 533, Hogye-dong, Dongan-gu, Anyang-shi, Kyongki-do, 431-749, Korea, E-mail: dseo@lge.com

School of Electrical Engineering, Seoul National University
Shinlim-dong, Kwanak-gu, Seoul 151-742, Korea
E-mail: shmin@mobile.snu.ac.kr, klee@snu.ac.kr, ylee@snu.ac.kr

ABSTRACT

Recently, a new direction of arrival (DOA) estimation scheme, direction lock loop (DiLL) was proposed in [6-7]. It is configured to operate in noncoherent mode, in other words, it uses an amplitude squaring of the spatial correlator output. As a result, there is squaring loss due to amplitude squaring in noncoherent DiLL (N-DiLL).

In this paper, a new DOA estimation scheme, coherent DiLL (C-DiLL), is proposed. The C-DiLL utilizes the real part of the spatial correlator output, and its performance is better than that of the N-DiLL. The use of the real part in the C-DiLL makes it possible that two branches of spatial correlators in the N-DiLL are merged to one branch. However, the C-DiLL needs to estimate carrier phase and transmitted data.

The DOA estimation accuracy and tracking capability of the C-DiLL are investigated by computer simulations, in comparison with those of the noncoherent DiLL.

I. Introduction

The growing demand for wireless multimedia services requires reliable and high data rate communications over wireless channel. However, since the frequency resource is scarce, spectrally efficient communication techniques are needed. Smart antenna systems have attracted great interest in recent years as a potential solution to this problem [1]. When smart antenna systems are appropriately used in wireless communication systems, they may improve system capacity by steering a beam to the desired signal and nulls to interferences [1-3].

The direction of arrival (DOA) is one of the useful information in the smart antenna system. The DOA information may be used in the downlink beamforming as well as uplink beamforming [2]. A large number of DOA estimation methods are listed in [4]. Two typical DOA estimation methods are Multiple signal classification (MUSIC), and Estimation of signal parameters via rotational invariance technique (ESPRIT). These methods are based on eigen analysis which requires significant computation. To overcome this problem, the projection approximation subspace tracking with deflation (PASTd) method for signal subspace update has been proposed by Yang [5].

Recently, a new DOA estimation scheme named direction lock loop (DiLL) was proposed in [6-7]. The DiLL estimates the DOA of a signal by using an error signal. The error signal is generated by taking the difference between the amplitude square values of two spatial correlator outputs. The amplitude squaring operations eliminate the need for carrier recovery. The spatial correlator outputs are obtained by correlating an input signal with the array response vectors whose directions are $+\Delta\theta$ and $-\Delta\theta$ shifted from the DOA estimate. In addition, the DiLL can track the DOA of a moving source, because the DOA estimate is updated iteratively.

In this paper, to improve performance, we propose a new DOA estimation scheme, coherent DiLL (C-DiLL), which generates an error signal from the real parts of two spatial correlator outputs, instead of the amplitude square values. In addition, the real operation makes it possible that two branches of spatial correlators are combined to one branch as in a coherent DLL in [8]. However, the carrier recovery and the transmitted data estimation are required.

The remainder of this paper is organized as follows. In the next section, we present the system model considered in this paper. The configuration and characteristics of the proposed C-DiLL are presented in Section III. The numerical results for the performance of C-DiLL are shown in Section IV, and the conclusions are given in Section V.

II. System Model

Consider a uniform linear array with N sensors, spaced by half wavelength distance. For comparison with N-DiLL in [7], a single user case is investigated. The transmitted signal bandwidth is assumed to be narrow enough. The down-converted signal vector, received by antenna elements at the ith time, may be represented as

$$\mathbf{r}(i) = \mathbf{a}(\theta)e^{j\phi_e}d(i) + \mathbf{v}(i), \quad (1)$$

where $\mathbf{r}(i) = [r_1(i), \cdots, r_j(i), \cdots, r_N(i)]^T$, and $r_j(i)$ is a received signal at the jth antenna. $\mathbf{a}(\theta) = [e^{j0} \quad e^{j\pi\sin\theta} \quad \cdots \quad e^{j(N-1)\pi\sin\theta}]^T$ represents an array response vector for a signal with DOA θ. ϕ_e is the carrier phase error introduced by the imperfect carrier recovery, and $d(i)$ is a source signal at time i and assumed to be $|d(i)|^2 = 1$ for simplicity. $\mathbf{v}(i)$ is an additive spatially and temporally white Gaussian noise vector with covariance matrix $\sigma^2\mathbf{I}$, where σ^2 is the noise variance.

III. Coherent DiLL

In this section, we present the C-DiLL, and investigate the characteristics of the C-DiLL in comparison with the N-DiLL.

A. Coherent DiLL system configuration

0-7803-7488-6/02/$17.00 © 2002 IEEE.

To improve performance, an error signal needed in updating the DOA estimate may be generated from the real part of the correlator outputs instead of the amplitude square [8]. The block diagram of the C-DiLL is shown in Fig. 1. The structure of the C-DiLL generally resembles that of the coherent DLL for timing synchronization. The C-DiLL uses the real part of the spatial correlator output, while the N-DiLL does the amplitude square of the spatial correlator output. The C-DiLL needs carrier recovery and transmitted data estimation.

The received signal vector $\mathbf{r}(i)$ is multiplied by a conjugate of transmitted data estimate $\hat{d}^*(i)$ to remove the effect of $d(i)$, and then spatially correlated with a difference of two array response vectors which are $+\Delta\theta$ shifted and $-\Delta\theta$ shifted relative to the DOA estimate $\hat{\theta}$, respectively. On the assumption of no carrier phase error and error-free data estimate, $\phi_e = 0$ and $\hat{d}(i) = d(i)$, the spatial correlator output may be represented as

$$z_c(i) = \frac{\hat{d}^*(i)}{N}\left(\mathbf{a}^H(\hat{\theta}(i)+\Delta\theta) - \mathbf{a}^H(\hat{\theta}(i)-\Delta\theta)\right)\mathbf{r}(i) \quad (2)$$
$$= R(\theta,\hat{\theta}(i)+\Delta\theta) - R(\theta,\hat{\theta}(i)-\Delta\theta) + v_c(i)$$

where the normalized spatial correlation function $R(\theta_1,\theta_2)$ is defined as $R(\theta_1,\theta_2) = \frac{1}{N}\mathbf{a}^H(\theta_2)\mathbf{a}(\theta_1) = \frac{1}{N}\sum_{n=1}^{N} e^{j\pi(n-1)(\sin\theta_1-\sin\theta_2)}$, and the noise term $v_c(i)$ is expressed as $v_c(i) = \frac{\hat{d}^*(i)}{N}\left(\mathbf{a}^H(\hat{\theta}(i)+\Delta\theta) - \mathbf{a}^H(\hat{\theta}(i)-\Delta\theta)\right)\mathbf{v}(i)$. The superscripts * and H denote the complex conjugate and Hermitian transpose, respectively.

The real part of the spatial correlator output forms an error signal,

$$e_c(i) = \mathrm{Re}(z_c(i)) = G_c\left(\hat{\theta}(i)|\theta\right) + v_{ec}(i), \quad (3)$$

where

$$G_c\left(\hat{\theta}(i)|\theta\right) = \mathrm{Re}\left(R(\theta,\hat{\theta}(i)+\Delta\theta) - R(\theta,\hat{\theta}(i)-\Delta\theta)\right), \quad (4)$$

and $v_{ec}(i) = \mathrm{Re}(v_c(i))$. The plot of $G_c\left(\hat{\theta}(i)|\theta\right)$ is referred to the S-curve because of the shape, as shown in Fig. 2 (a).

The error signal is filtered and fed to the numerically controlled oscillator (NCO) to update the DOA estimate iteratively. The DOA estimate at the $(i+1)$th time is updated using the following adaptive equation,

$$\hat{\theta}(i+1) = \hat{\theta}(i) + K_0 \cdot (\hat{e}_{mc}(i) \otimes f(i)), \quad (5)$$

where $\hat{e}_{mc}(i)$ is the estimated modified error signal, $f(i)$ is the impulse response of the loop filter, K_0 is the NCO gain, and $\otimes$ denotes convolution. The iterative updating of DOA estimate enables the C-DiLL to track the DOA of a moving source by iterations.

B. Modification factor

To get a correct DOA estimate, $G_c\left(\hat{\theta}|\theta\right)\Big|_{\hat{\theta}=\theta}$ in (3) should be zero. In other words, the error signal should be zero, when $\hat{\theta}$ is equal to θ. However, since $G_c\left(\hat{\theta}|\theta\right)\Big|_{\hat{\theta}=\theta}$ is not generally zero, the DOA estimate has a bias. The error signal should be corrected by subtracting a modification factor, which is represented as

$$e_{mc}(i) = \mathrm{Re}(z_c(i)) - m_c(\theta(i)), \quad (6)$$

where the modification factor $m_c(\theta)$ is defined as

$$m_c(\theta) = G_c(\theta|\theta) = \mathrm{Re}(R(\theta,\theta+\Delta\theta) - R(\theta,\theta-\Delta\theta)). \quad (7)$$

However, the exact value of θ required in (7) is not available. θ is replaced by the estimated value, $\hat{\theta}$, and (6) is modified to

$$\hat{e}_{mc}(i) = \mathrm{Re}(z_c(i)) - m_c\left(\hat{\theta}(i)\right) = G_{mc}\left(\hat{\theta}(i)|\theta\right) + v_{ec}(i) \quad (8)$$

where

$$G_{mc}\left(\hat{\theta}(i)|\theta\right) = G_c\left(\hat{\theta}(i)|\theta\right) - m_c\left(\hat{\theta}(i)\right). \quad (9)$$

C. Characteristics of the C-DiLL

The negative slope value of $G_{mc}\left(\hat{\theta}(i)|\theta\right)$ ensures that the DOA estimate converges to an actual DOA θ, when the initial DOA estimate is in a locking range [7]. The locking range $(\theta_{zc-}, \theta_{zc+})$ is defined as the range between the two zero crossing points of $G_{mc}\left(\hat{\theta}(i)|\theta\right)$ which are closest to $\hat{\theta} = \theta$ on the left and right sides. Fig. 2 (a) shows $G_{mc}\left(\hat{\theta}(i)|\theta\right)$ of the C-DiLL and N-DiLL as a function of $\hat{\theta}$, when N=4, K_0=0.05, and θ=0°.

Since θ_{zc-} and θ_{zc+} are difficult to be expressed in closed forms, these values are approximated as θ_- and θ_+. θ_- is the negative zero crossing point of $\mathrm{Re}\left(R(\theta,\hat{\theta}(i)+\Delta\theta)\right)$ nearest to $\hat{\theta}=\theta$, and θ_+ is the positive zero crossing point of $\mathrm{Re}\left(R(\theta,\hat{\theta}(i)-\Delta\theta)\right)$ nearest to $\hat{\theta}$=0°. θ_- and θ_+ can be calculated from the following equations

$$\pi(\sin(\theta) - \sin(\theta_+ - \Delta\theta)) = -\frac{\pi}{N-1}. \quad (10)$$
$$\pi(\sin(\theta) - \sin(\theta_- + \Delta\theta)) = \frac{\pi}{N-1}$$

It is found that $G_{mc}\left(\hat{\theta}(i)|\theta\right)$ has a zero value when $\hat{\theta}$ = ±90°. Then, we may express the approximated values of θ_{zc-} and θ_{zc+} as follows,

$$\theta_{zc,+} \approx \min\left(\sin^{-1}\left(\sin(\theta) + \frac{1}{N-1}\right) + \Delta\theta, 90^\circ\right)$$
$$\theta_{zc,-} \approx \max\left(\sin^{-1}\left(\sin(\theta) - \frac{1}{N-1}\right) - \Delta\theta, -90^\circ\right) \quad (11)$$

Comparing (11) with (9) in [7], it is found that the locking range of the C-DiLL is equal to or narrower than that of the N-DiLL, when $N \geq 2$.

IV. Numerical Results

In this section, we compare the performance of the C-DiLL with that of the N-DiLL. In Subsections A and B, it is assumed that the estimations of the carrier phase and transmitted data are exact. Since it is not possible to estimate the carrier phase and transmitted data exactly, the effects of carrier phase estimation error and data estimation error are investigated, in the Subsection C.

The parameters used in these numerical results are N=8, K_0=0.05, and $F(z)=\frac{0.1}{1-0.9z^{-1}}$.

A. DOA error variance

In Fig. 3, we investigate the DOA error variances of the C-DiLL in a steady state and compare its results with those for the N-DiLL. Fig. 3 shows the DOA estimation error variance as a function of SNR, when θ=18°, and $\Delta\theta$ is set to 5.09° for C-DiLL and 6.01° for N-DiLL. It is observed that the C-DiLL requires 3.5 dB less SNR than the N-DiLL for the same DOA estimation error variances, and the analysis agrees well with the simulation results marked with the symbol, 'X'. These results may be interpreted that there is no performance degradation due to squaring loss in the C-DiLL.

B. Tracking capability

In addition to the DOA error variance, the tracking capability is considered to be another important performance measure of the DiLL. As stated in [7], there is trade-off between DOA estimation accuracy and tracking capability. Fig. 4 shows both the trajectory of θ for a moving signal source over time, and the mean square errors of N-DiLL and C-DiLL, obtained by ensemble averaging over 1000 independent trials. We include an additional case of N-DiLL, where the NCO gain K_0 is set to 0.0228 to make the DOA error variances at θ=0° be the same as that of the C-DiLL. SNR is set to 10dB, and $\Delta\theta$ is the same as in Fig. 3. $\theta(i)$ is set to 0° during 160 symbol times, and then is varied with time i, as $\theta(i)=80\sin((i-161)/1000)°$. It is found that C-DiLL has less mean square error for the DOA of a moving signal source, when both DiLLs have the same parameter K_0.

In comparison of the C-DiLL and the N-DiLL with K_0=0.0228, both have the same mean square errors during the first 160 symbols because θ is fixed, and then the differences of mean square errors between both DiLLs start to appear after θ varies. The sudden fluctuations occur because of angular velocity change of θ at the 161st symbol time. As θ goes far from 0°, the difference of the mean square error of DiLLs increases. However, the mean square errors are almost the same where the angular velocity of θ approaches to 0°. From these results, we may conclude that the C-DiLL has better tracking performance than the N-DiLL when both have the same DOA estimation error variance.

C. Effects of phase error and data estimation error

The effects of the carrier phase error and data estimation error on the DOA estimation are presented in Fig. 5. The DOA of a signal θ is set to 18°, SNR is 10dB, and $\Delta\theta$ is the same as used in Fig. 3. The carrier phase error, ϕ_e's in (1) are assumed to be Gaussian distribution. Fig. 5 (a) shows the DOA error variance as a function of standard deviation of carrier phase error. The performance of the N-DiLL does not vary with the carrier phase error, whereas that of the C-DiLL varies becauses of the decrease in the power of the real part of the spatial correlator output. The C-DiLL has smaller DOA error variance than the N-DiLL, when the standard deviation is less than 6°. Fig. 5 (b) shows the DOA error variance as a function of data estimation error rate. The C-DiLL has smaller DOA error variance than the N-DiLL, when the data estimation error is less than 15%.

V. Conclusions

In this paper, the coherent direction lock loop (C-DiLL) is proposed for direction of arrival (DOA) estimation. The C-DiLL estimates the DOA of a signal by using the error signal from the real part of the spatial correlator output. In the C-DiLL, two spatial correlator branches in the N-DiLL can be combined to one branch.

The numerical results from analysis and simulations show that the C-DiLL requires 3.5dB smaller SNR for the same error variances than the noncoherent DiLL. This is because the squaring loss does not exist in the C-DiLL. The C-DiLL tracks better than the N-DiLL for a moving source. The performance of the C-DiLL is found to degrade in the presence of phase estimation error and data estimation error. However, the C-DiLL has smaller error variance than the N-DiLL, when the standard deviation of the carrier phase error is less than 6° or the data estimation error is less than 15%.

References

[1] G. V. Tsoulos, "Smart Antennas for Mobile Communication Systems: Benefits and Challenges," *Electronics & Communication Engineering Journal*, Vol.11 Issue 2, pp. 84-94, April 1999.

[2] L. C. Godara, "Application of Antenna Arrays to Mobile Communications, Part I: Performance Improvement, Feasibility, and System Considerations," *Proc. IEEE*, vol. 85, no. 7, pp. 1031-1060, Jul 1997.

[3] J. C. Liberti, Jr. and T. S. Rappaport, *Smart Antennas for Wireless Communications: IS-95 and Third Generation CDMA Applications*, Prentice Hall, NJ, 1999.

[4] L. C. Godara, "Application of Antenna Arrays to Mobile Communications, Part II: Beam-Forming and Direction-of-Arrival Considerations," *Proc. IEEE*, vol. 85, no. 8, pp. 1195-1245, Aug. 1997.

[5] B. Yang, "Projection Approximation Subspace Tracking," *IEEE Trans. Signal Processing*, vol. 43, no. 1, pp. 95-107, Jan. 1995.

[6] W. Hou and H. M. Kwon, "Interference suppression receiver with adaptive antenna array for code division multiple access communications systems," Proceedings in *IEEE Vehicular Technology Conference 2000*, Sep. 2000.

[7] S. Min, K. B. Lee, and Y.-H. Lee, "'Direction of Arrival' Estimation Algorithm: Direction Lock Loop," *Proceedings in CDMA International Conference*, Nov. 2001.

[8] R. de Gaudenzi, and M. Luise, "Decision-Directed Coherent Delay-Lock Tracking Loop for DS-Spread-Spectrum Signals," *IEEE Trans. Commun.*, vol. 39, no. 5, May 1991.

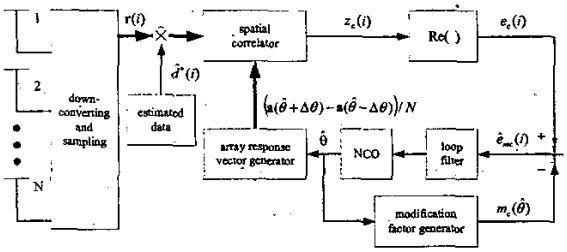

Fig. 1. Coherent DiLL block diagram

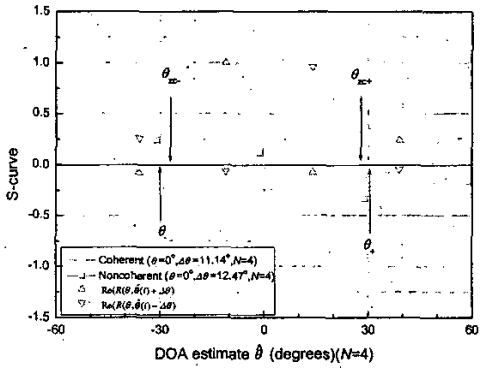

Fig. 2. S-curve

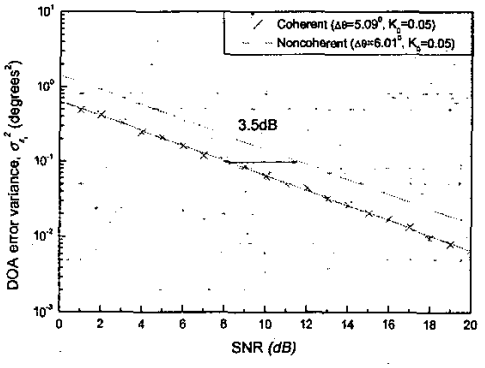

Fig. 3. DOA estimation variances as a function of SNR

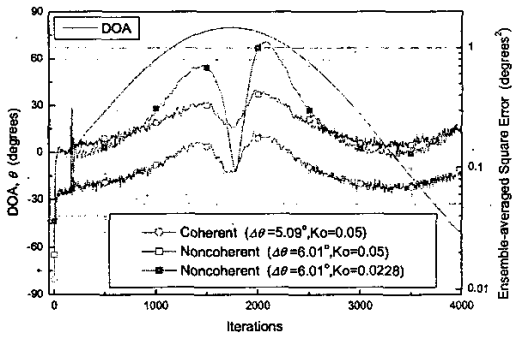

Fig. 4. DOA tracking

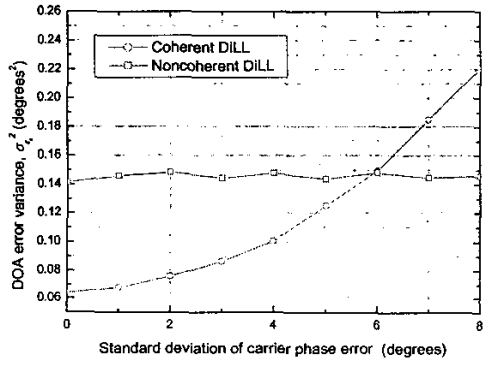

(a)

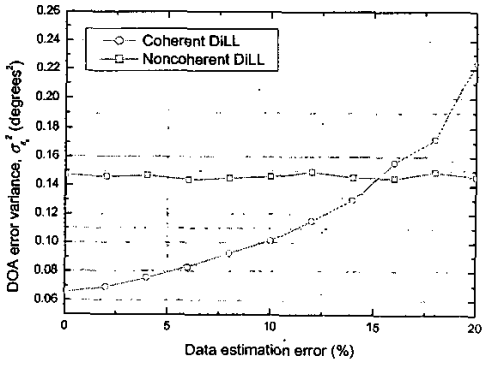

(b)

Fig. 5. Effects of carrier phase error and data estimation error